ACS OMEGA

Open Access

http://pubs.acs.org/journal/acsodf

Article

Preadsorbed Chymotrypsin Modulated the Composition of Protein Corona and Immunological Response

Ling Han,* Yijing Wang, Hongyan Jia, Zhiqin Zhang, Shouning Yang, Fangxiao Li, Fengfeng Li, and Huayan Yang*

Cite This: *ACS Omega* 2024, 9, 27898−27905

Read Online

ACCESS | Metrics & More | Article Recommendations

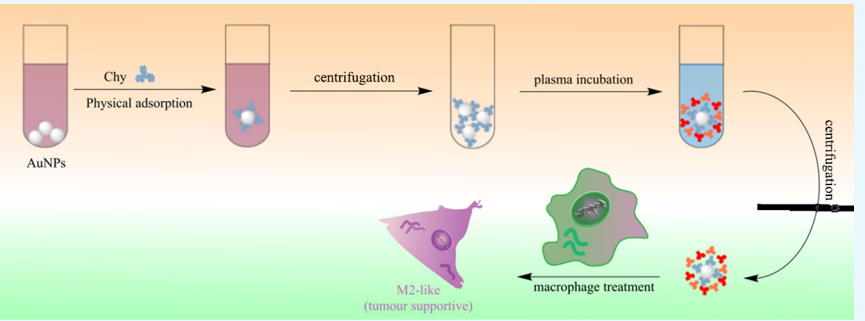

ABSTRACT: It is well-known that proteins after administration into biological environments adsorb on the surface of nanoparticles (NPs). The biological identity could be determined by protein corona, but whether and how the preadsorbed molecules impact the composition of the corona and immunological response have rarely been reported. Here, the effects of preadsorbed chymotrypsin (Chy) on forming protein corona and subsequent immunological response are reported. We find that preadsorbed Chy on the surface of AuNPs results in a protein corona with enriched immunoglobulins and reduced human serum albumin protein, which further affect the polarization of macrophages into specific phenotypes. Our study suggests that the protein surrounding the nanoparticles could affect the protein corona and immunological response, which may direct the preparation of multifunctional nanomedicine for future studies.

1. INTRODUCTION

When exposed to blood, nanoparticles (NPs) will inevitably interact with biomolecules and form a "protein corona" on their surface. Increasing evidence show that protein corona has an important influence on the bioavailability of nanomedicines.[1−5] Many factors such as the size, shape, and physicochemical properties of NPs affect the formation of protein corona.[6,7] Thus, the surface chemistry on NPs modulates the formation of a protein corona as a critical consideration. Therefore, understanding the role of surface binding techniques on how to form the protein corona is a prerequisite toward the safe and efficacious clinical application of nanomedicines.[7−817]

Because of increasing contact with nanomaterials, the effects of nanoparticles on macrophages deserve particular attention.[18] Macrophage is a part of the immune system that phagocytoses foreign antigens. However, macrophages could be polarized into the M1 phenotype or the M2 phenotype by exposure to diverse stimuli, and M1 and M2 phenotype macrophages play distinct roles in many situations. M1 macrophages are often thought of as tumor-killing macrophages, primarily antitumor and immune-boosting. On the other hand, M2 macrophages are immunosuppressed, promoting tissue repair and regulating inflammation. Surface-modified nanoparticles have been shown to modulate macrophage polarization.[19,20] Specifically, the surface chemistry on NPs could impact the formation of the protein corona and then determine nanoparticle targeting and immune responses.[21−222324252627282930313233343536 37]

Gold nanoparticles (AuNPs) have been widely studied in the nanobiomedicine field in the past decade.[1−4] Especially, AuNPs have been identified as excellent photothermal therapy agents for tumor treatment[5−8] as well as CT imaging reagents for cancer diagnosis[14,15] as well as treatment platforms for drug loading and release.[16] However, AuNPs displayed severe toxicity toward cells, larval zebrafish, etc.,[4,9] indicating noteworthy toxicity issues of AuNPs in biological applications. The following studies show that the protein corona, which is

Received: October 21, 2023
Revised: December 25, 2023
Accepted: January 3, 2024
Published: June 17, 2024

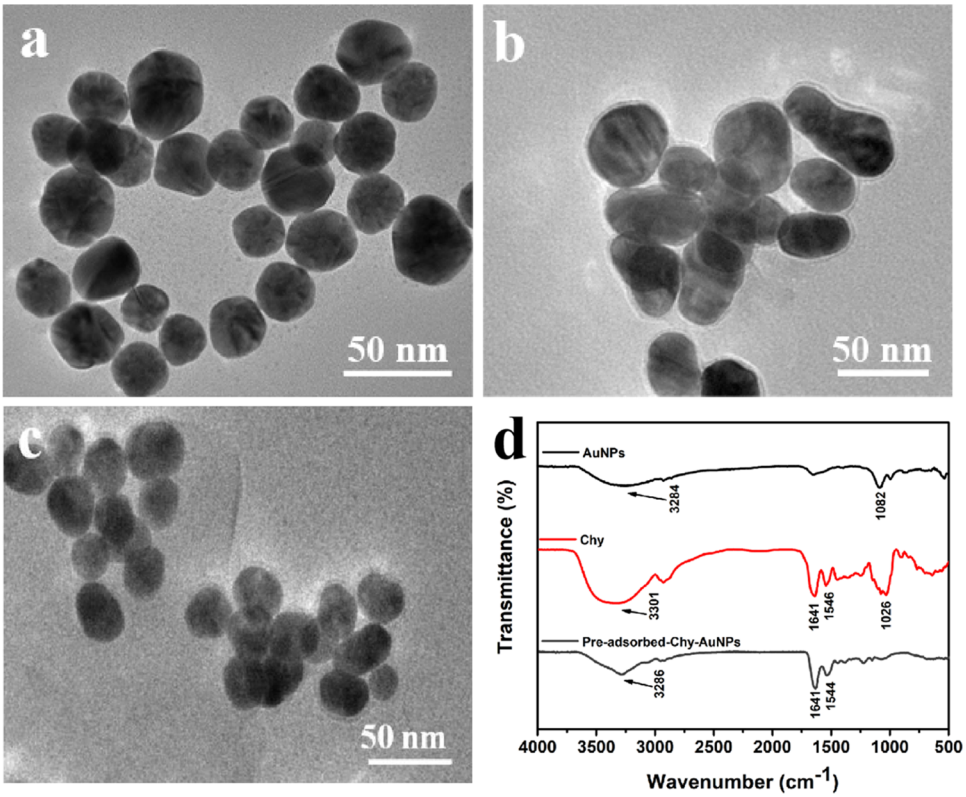

Figure 1. Transmission electron microscopy image from three kinds of AuNPs. (a) AuNPs, (b) preadsorbed-Chy-AuNPs, and (c) protein corona on the surface of preadsorbed-Chy-AuNPs. (d) Fourier transform infrared spectroscopy (FT-IR) of the obtained Chy, AuNPs, and preadsorbed-Chy-AuNPs.

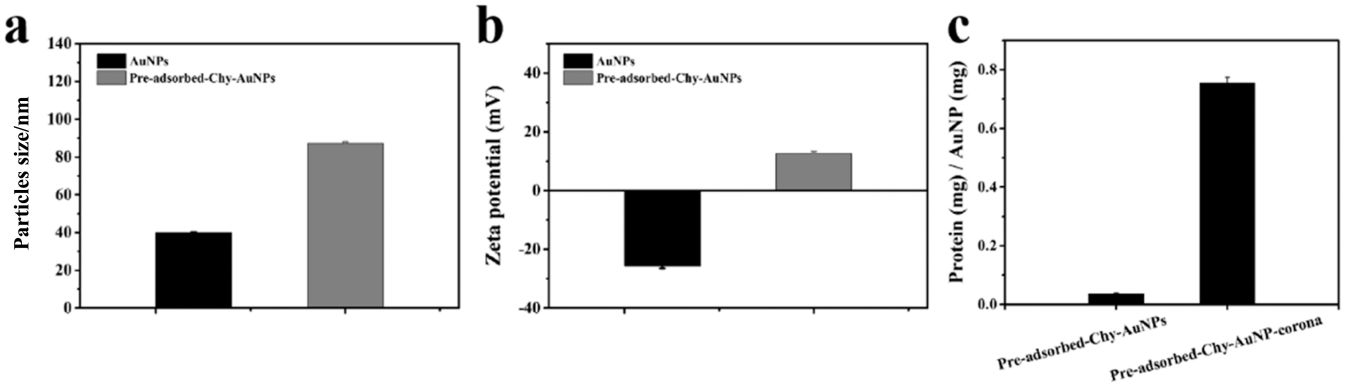

Figure 2. (a) Hydrodynamic diameters and (b) ζ-potentials of the obtained AuNPs and preadsorbed-Chy-AuNPs. (c) Bicinchoninic acid (BCA) quantification of protein on the surface of preadsorbed-Chy-AuNPs.

on the surface of NPs, could alter the toxicity[10] of NPs. Moreover, more studies also found that the protein corona could regulate the polarization of macrophages to either proinflammatory (M1) phenotype or anti-inflammatory (M2) phenotype.[7,12] However, the natural corona formed by unconditional contact between NPs and plasma proteins has a variable impact on macrophage polarization due to the instability of protein corona components.[13] Therefore, it is highly desired to develop a new method that could directionally polarize macrophages into a definite phenotype. In this work, a convenient method was developed to decorate AuNPs for inducing macrophages directionally into the M2 phenotype. After a systematic screening, we found that the coating of chymotrypsin on the surface of AuNPs can affect the adsorption of plasma proteins, thereby regulating the polarization of macrophages. Moreover, combined proteomics techniques were used to elucidate the corona, and enriched immunoglobulins (Igs) were observed when compared to pristine AuNP-corona. In a word, our findings demonstrate that the cladding of protein on the surface could affect the deposition of plasma protein and further regulate the immunological response of nanoparticles.

2. RESULTS AND DISCUSSION

2.1. Physicochemical Properties of Preadsorbed-Chy-AuNPs. AuNPs were prepared with gold chloride and sodium citrate by using water as the solvent. The image of representative transmission electron microscopy (TEM) is shown in Figure 1a. The size of the primary particle was found

https://doi.org/10.1021/acsomega.3c08288
ACS Omega 2024, 9, 27898−27905

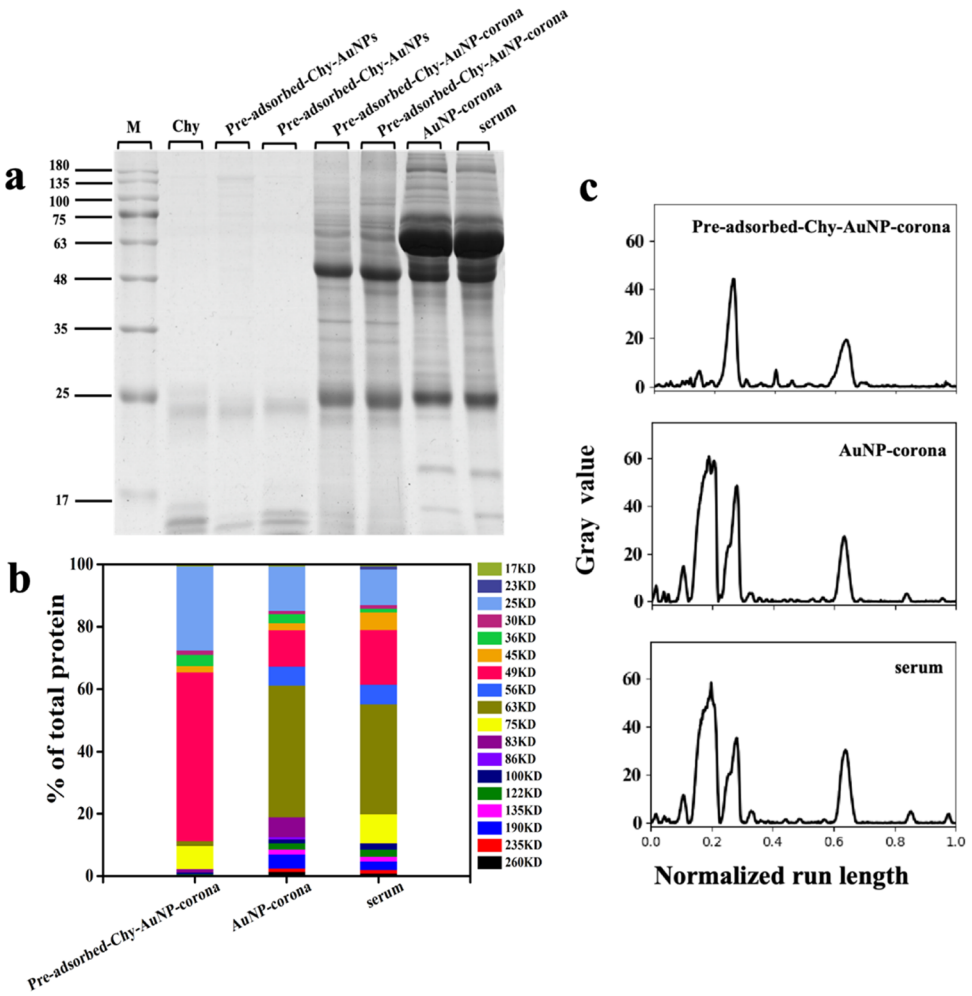

Figure 3. (a) SDS-PAGE visualizing the quantities and the kinds of proteins forming on AuNP-corona and preadsorbed-Chy-AuNPs. (b) Band intensities of adsorbed proteins on NPs. (c) Profile GE Image Quant TL on the basis of their gray values.

to be 38 nm from the TEM image. The preadsorbed Chy on AuNPs is shown in Figure 1b, and the Chy thickness was found to be 2.5 nm. Figure 1c shows the preadsorbed-Chy-AuNP-protein corona, which was prepared by incubating the preadsorbed-Chy-AuNPs with plasma for 12 h and centrifuged for separation.

The comparison of the FT-IR peaks for AuNPs and preadsorbed-Chy-AuNPs is shown in Figure 1d, which confirms the deposition of protein on the surface of AuNPs. From the IR spectra of proteins, we found that vibrational bands, which are the most prominent, were amide I bands (1700−1600 cm^{-1}) and amide II bands (~1550 cm^{-1}).[18] The vibrational location of the amide I bands is determined by the nature of the hydrogen band from the C−O and NH moieties.[38] The characteristic band of the C−O stretching vibrations is shown as amide II bands.[38] Therefore, the peaks at 1546 and 1641 cm^{-1} could be assigned to the IR vibration of preadsorbed-Chy-AuNPs.

Dynamic light scattering (DLS) and ζ-potential further characterized the preadsorbed-Chy-AuNPs. As shown in Figure 2a, the hydrated diameter of preadsorbed-Chy-AuNPs was 87 ± 0.62 nm. The complex of AuNP-chymotrypsin aggregating together with proteins may cause the hydrated diameters to increase. As shown in Figure 2b, in water, the ζ-potential values from the AuNPs were (−25.9 ± 0.70 mV), while chymotrypsin was preadsorbed on the surface of AuNPs, and the ζ-potential was changed to be 12.5 ± 0.21 mV. The results indicated the changes on the surface of nanoparticles.

The amount of chymotrypsin adsorbed on the surface of AuNPs was determined by a Bradford protein assay kit, with calculations of samples based on the standard curve. From Figure 2c, we can see that 0.04 mg of protein/1 mg of AuNP proteins was adsorbed on the surface of preadsorbed-Chy-AuNPs. NPs were incubated with plasma pooled from three healthy donors and separated by centrifugation. Preadsorbed-Chy-AuNPs were also incubated with plasma; after centrifugation, preadsorbed-Chy-AuNP-corona was separated via removing the supernatant. We found that 0.76 mg of protein/1 mg of AuNP of proteins was adsorbed on the surface of preadsorbed-Chy-AuNPs.

2.2. Composition of Protein Corona on the Surface of Preadsorbed-Chy-AuNPs. The major components of the protein corona on the surface of AuNPs and preadsorbed-Chy-AuNPs could be visualized by sodium dodecyl sulfate-polyacrylamide gel electrophoresis (SDS-PAGE) (Figure 3). The protein coronas were treated with SDS-Tris-HCl buffer according to the method reported in the literature.[18] As shown in Figure 3, different types and densities of proteins among the NP-corona complexes constitute the coronas. From Figure 3a, we found that the quantities and the kinds of proteins adsorbed by AuNPs are very different from preadsorbed-Chy-AuNPs.

https://doi.org/10.1021/acsomega.3c08288
ACS Omega 2024, 9, 27898−27905

Table 1. Identified Corona Proteins Binding to AuNPs and Preadsorbed-Chy-AuNPs after Incubation[a]

accession number	protein name	MW (kDa)	function
P68871	hemoglobin subunit	17,102	oxygen transport
P19652	α-1-acid glycoprotein 2	23,588	related to acute phase response
P02647	apolipoprotein A-I	30,759	metabolism
P0C0L4	complement C4-γ	33,130	immune response
P01859	immunoglobulin heavy constant γ2	35,878	immune response
P01861	immunoglobulin heavy constant γ-4	35,918	immune response
P01857	immunoglobulin heavy constant γ1	36,083	immune response
P01877	immunoglobulin heavy constant α-2	36,503	immune response
P00738	haptoglobin	45,177	modulate acute phase response
P01871	immunoglobulin heavy constant	49,276	immune response
P02675	fibrinogen β chain	56,577	immune response, coagulation
P02768	serum albumin	66,500	osmotic pressure
P02787	serotransferrin	75,100	transport
P00488	coagulation factor XIII A chain	83,728	participate in blood clotting
P06396	gelsolin	86,034	peptidase
Q6NZF1	zinc finger CCCH domain-containing protein	106,316	transport
P00450	ceruloplasmin	122,128	iron transport
P01023	α-2-macroglobulin	163,188	immune response
P01024	complement C3	187,030	immune response
P02751	fibronectin	262,460	growth, migration, and differentiation

[a]Plasma proteins were determined by matrix-assisted laser desorption ionization-time of flight mass spectrometry (MALDI-TOF-MS) (proteome analysis) and reproducibly investigated on SDS gels.

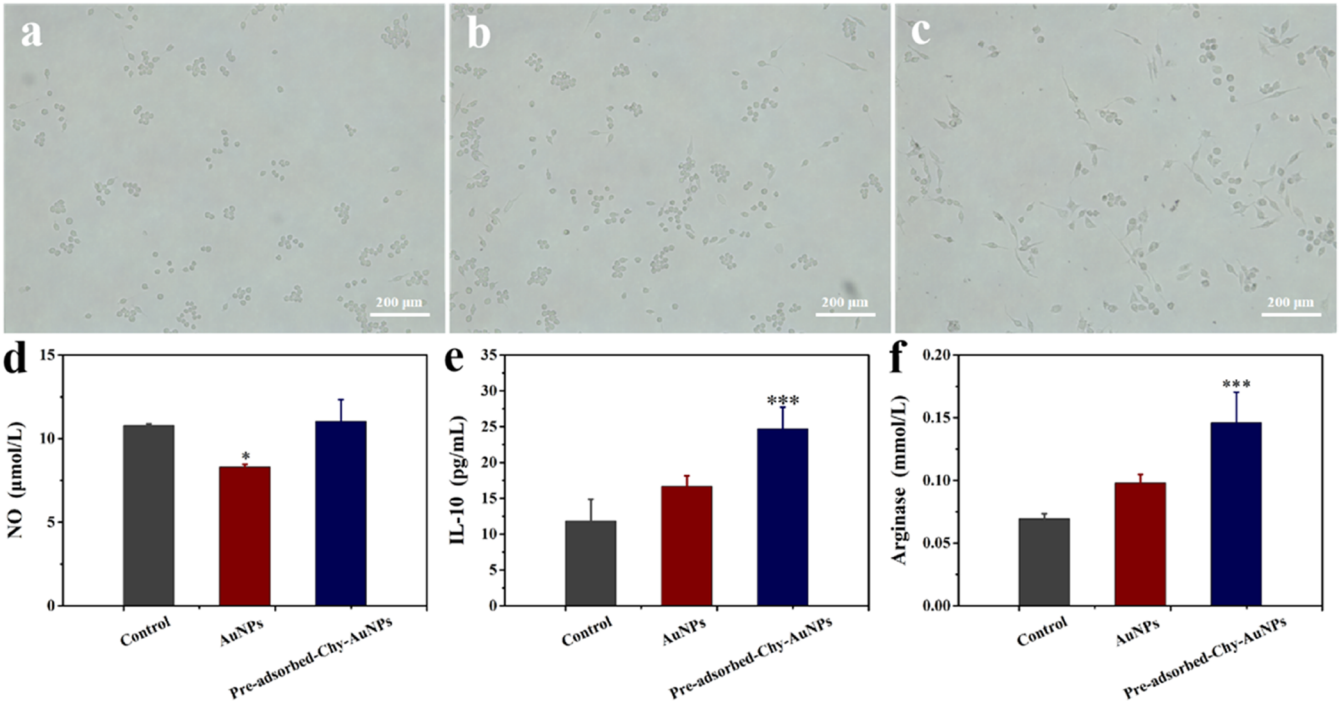

Figure 4. (a–c) Macrophage morphology activated by control (without NPs), AuNPs, and cells treated with the AuNP-protein complex. (d–f) Expression via iNOS, IL-10, and arginase-1 according to control (without NPs), AuNPs, and AuNP-protein complex. Error bars represent the standard error of the mean (SEM) ***$p < 0.001$ compared to control cells, which was determined by our test.

GE Image Quant TL (Figure 3b) is another method to analyze the different amounts of protein that are adsorbed by NPs. The banding pattern showed that most of the total intensity of corona in the serum and Au-corona was contributed by 63 kDa, the most abundant protein. Around 48, 25, 56, 68, and 100 kDa, the bands were shown to have lower abundant proteins (Figure 3b). In the proteins adsorbed on preadsorbed-Chy-AuNPs, the most abundant proteins were around 48 and 25 kDa. 68, 30, 36, and 100 kDa made a smaller contribution to the total corona intensity. From the results, it can be seen that the change in surface functionalization of the NPs may induce different biological responses.

Next, liquid chromatography-mass spectrometry (LC–MS) results confirmed that the peptide sequences and trypsin digested the selected SDS-PAGE bands. In Table 1, a library of 20 proteins in coronas is listed, containing highly abundant proteins (e.g., immunoglobulins [Igs], apolipoprotein [Apo], and human serum albumin [HSA]) and low-abundance

https://doi.org/10.1021/acsomega.3c08288
ACS Omega 2024, 9, 27898–27905

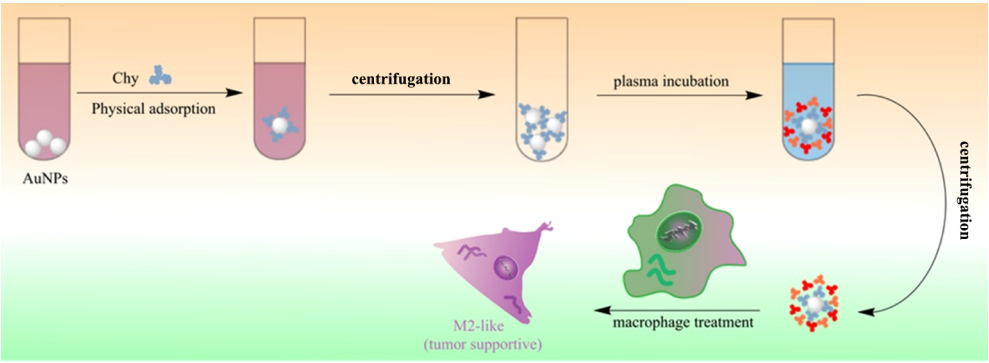

Figure 5. Schematic diagram of the AuNP-protein complex coincubated with macrophage cells. Preadsorption of AuNPs was performed through incubation with plasma and then pelleted from the supernatant through centrifugation. After washing, the AuNP-protein complex was treated with macrophage cells for 24 h.

proteins (e.g., gelsolin and zinc finger CCCH domain-containing protein) in blood. Most of the proteins are highly abundant in blood (e.g., human serum albumin [HSA], apolipoprotein [Apo], and immunoglobulins [Igs]), whereas some of them are low abundance proteins in blood (e.g., zinc finger CCCH domain-containing protein and gelsolin). From Figure 3c, we can see that complement proteins (~189 kDa), HSA (~66.5 kDa), and Ig (~48 kDa) were detected in Au-coronas, while Ig (~48 kDa) and fibronectin (~26 kDa) comprised the majority of the preadsorbed-Chy-AuNPs. HSA (~66.5 kDa) was also detected in CHY-AuNP-corona, only occupying a small proportion. The adsorption of apolipoprotein A-I, haptoglobin, and zinc finger CCCH domain-containing protein was also detected in CHY-AuNP-corona; these proteins are related to immune response and may cause reversal of macrophage polarization.

2.3. Constituent Analysis of the Protein Corona. 2.4. Induction of the Polarization of Macrophages and Cytokine Release. Recently, cell morphology was reported as an indicator of cell phenotype,[39] and the morphology of macrophages was assessed using RAW 264.7 cells as a model cell line via AuNPs and activation of preadsorbed-Chy-AuNPs. The macrophage polarization state is related to changes in cell shape.[40] The iconic morphology of macrophages in the polarization state is monitored as two types: cells in the M1 phenotype are rounded and cells in the M2 state are elongated. The main thing that distinguishes M1 from M2 is that the degree of cell elongation is monitored (length of the longest axis divided by the length of the short axis across the cell nucleus).[40,41] From Figure 4a,b, the control group without NP was detected as round-shaped cells, which was consistent with the reported literature.[18] The incubated macrophages with preadsorbed-Chy-AuNPs caused more than 80% of the cells to have obvious pseudopods and elongated shapes (Figure 4c). The cell elongation may have an influence on programs of genetic association with macrophage phenotype.

The expression using arginase-1 and inducible nitric oxide synthase was also evaluated in order to distinguish the M1/M2 polarization state of macrophage stimulated by preadsorbed-Chy-AuNPs; these methods are usually used as biomarkers of M1 and M2 macrophages.[42] Compared to the control groups, we found that AuNPs showed slightly lower iNOS levels (Figure 4d) and cells with preadsorbed-Chy-AuNP stimulation showed significantly higher levels of arginase (Figure 4f).

Further confirmation of polarization was evaluated by the levels of IL-10 (a cytokine secreted by M2 macrophages) in RAW 264.7 cells (Figure 4e). In comparison between the negative control groups and the AuNP-corona, cells treated with the preadsorbed-Chy-AuNPs released higher levels of IL-10, further confirming that they differentiated into the M2 phenotype. From the results, we found the preadsorbed-Chy-AuNP-treated cells were in the M2 polarization state (Figure 5). Chy predeposited on the surface of AuNPs changed the composition of the protein corona, subsequently inducing an immunological response, which provided insights into the clinical translation of nanomedicine.

3. CONCLUSIONS

In conclusion, we demonstrate that modifications of nanocarriers via adsorption of chymotrypsin can result in polarization of macrophages as the M2 phenotype. We also show that physical adsorption is a controlled way to form the protein corona. Some fundamental insights are provided by our study based on the complex influence on the protein corona, which is helpful to develop the safety of nanomaterials applied to medicine.

4. MATERIALS AND METHODS

4.1. Chemicals and Materials. *N*,*N*-Methylene bis-(acrylamide) methylene glycol and sodium citrate were ordered from Aladdin Reagent Co., Ltd. Au(III) chloride trihydrate was ordered from Chinese Sinopharm Chemical Reagent Co., Ltd. Ammonium bicarbonate (NH_4HCO_3), DL-dithiothreitol (DTT), *N*,*N*,*N*′,*N*′-tetramethylethylenediamine (TEMED), sodium dodecyl sulfate (SDS), and iodoacetamide (IAA) were ordered from Sigma-Aldrich. Coomassie brilliant blue R250, glycine, bromophenol blue, protein marker, tris(hydroxymethyl) aminomethane hydrochloride (TRIS-HCl), and Dulbecco's modified Eagle's medium (DMEM) without sodium pyruvate were ordered from Beijing Solaibio Co., Ltd. Methanol, ethyl alcohol absolute, and ammonium persulfate were ordered from Deen Chemical Reagent (Tianjin) Co., Ltd. Hydrochloric acid, acrylamide, glacial acetic acid, and glycerol were ordered from Tianjin Damao Chemical Reagent Co., Ltd. Acetonitrile (ACN) was ordered from Saan Chemical Technology (Shanghai) Co., Ltd. Sequencing-grade modified trypsin was ordered from Promega (Beijing) Biotech Co., Ltd. We used double-distilled water.

4.2. Preparation of AuNPs. The preparation of AuNPs was done according to a procedure published by Jana et al.[43] First, in a 500 mL three-necked round-bottom flask, sodium citrate solution (2 mL, mass fraction 1%) was added dropwise

https://doi.org/10.1021/acsomega.3c08288
ACS Omega 2024, 9, 27898−27905

to a solution of $HAuCl_4$ (200 μL, 0.1 g/mL) in H_2O (200 mL) with moderate stirring. Then, the reaction mixture was refluxed until a pink solution was detected. After that, the reaction mixture was quenched with ice water and centrifuged at 6000 rmp, and the AuNPs were separated, washed with deionized water three times, and then kept at 4 °C in a refrigerator for further use.

4.3. Preparation of Preadsorbed Chy on the Surface of AuNPs. *4.3.1. Physical Adsorption.* Proteins were physically immobilized on the surface of NPs, AuNPs (4 mg) were dispersed in phosphate-buffered saline (PBS) buffer (5 mL, 50 mM, pH 6), and then Chy (10 mg, 2 mg/mL) was added. After that, the mixture was incubated at room temperature for 6 h, and the preadsorbed-Chy AuNPs were separated and then washed twice with the deionized water and finally diluted to a final volume of 2 mL using distilled water.

4.4. Preparation of AuNP-Coronas. Preadsorbed-Chy AuNPs (8 mg) were added to 10% serum (7 mL), and the mixture was incubated with constant agitation at 37 °C for 6 h, forming the AuNP-coronas. The AuNP-coronas from the supernatant plasma (pelleted fraction) were separated using a centrifuge at 5000 rpm for 10 min. Subsequently, the resulting particles were washed with PBS (2 mL × 3 times) and resuspended in PBS (1 mL) for further use. We carried out three independent repetitions for separation.

4.5. Mass Spectrometry for Protein Identification.[44] The samples were added to 12% SDS-PAGE gel and maintained at 120 V for about 20 min until bromophenol blue below the stacking gel reached 1.5 cm. After that, according to the literature, a series of operations were performed on the entire protein-containing gel region, such as slice, reduction, alkylation, and finally in-gel digestion by trypsin.[45]

After trypsin digestion, the obtained solution (1 μL) was transferred to a MALDI plate and dried in air; then, HCCA (1 μL) was added and dried. Then, data were collected on the MALDI-TOF mass spectrometer (Bruker Daltonics) and searched using the Swiss-Prot master sequence database. The mass accuracy for the monoisotopic mass was set to 0.2 Da in the positive ion mode, and the method of unrestricted classification was used.

4.6. Cell Lines and Culture. The Shanghai Institute of Life Sciences provided the RAW 264.7 cell line. In a humidified atmosphere containing 5% CO_2, cells were cultured in a complete medium (DMEM, 100 U/mL penicillin, 10% fetal bovine serum [FBS], 100 μg/mL streptomycin, and 0.25 μg/mL amphotericin B) at 37 °C. The cells were washed with PBS four times before incubation with NPs or AuNP-coronas. Next, the preparation of Au-Chy (50 μg/mL) and stock solutions of AuNP-OVA were carried out in a complete medium. the medium containing NPs or NP-coronas was aspirated and discarded after culturing for another 24 h. The cells were separated and washed with PBS to remove NPs or NP-coronas that adhered to the surface of the cells loosely.[46,47] The macrophage morphology was examined using a Leica MC170 HD (Leica, Rijswijk, The Netherlands) to photograph the adherent cells.

The control experiments were performed without the addition of NPs or NP-corona using the same conditions.

4.7. Measurement of Nitric Oxide. First, in 6-well plates, 3.5×10^4 cells were cultured in a DMEM containing 10% FBS for 24 h. We carefully aspirated the medium and used PBS to wash the cells. Second, incubation of the cells with AuNPs or AuNP-coronas was done in a complete medium for another 24 h. The preparation of the control experiment was also done without the addition of NPs or NP-coronas using the same conditions. Based on the Griess reaction (US Everbright, Inc.), the nitrite content of the cells was analyzed by the nitric oxide (NO) method.[48] The detailed operation followed the manufacturing processes. Nitrite standard or culture supernatant (100 μL) was mixed with a Griess reagent (100 μL, the ratio of 0.1% *N*-[1-naphthyl-ethylenediamine dihydrochloride] in 2.5% phosphoric acid and 1% sulfanilamide is 1:1) in a 96-well plate. The absorbance at 540 nm was recorded by the multimode reader (EnVision, PerkinElmer) to quantify the NO amount produced by the RAW 264.7 cells.

4.8. Assay of Arginase. In 96-well plates, 3.5×10^4 cells were seeded and then incubated for 24 h in DMEM containing 10% FBS. We aspirated the medium carefully and used PBS to wash the cells. The incubation of the cells with AuNPs or AuNP-coronas was done in a complete medium for another 24 h after washing. The preparation of the control experiment was also done without the addition of NPs or NP-coronas using the same conditions. The supernatant (10 μL) was transferred to the enzyme-linked immunosorbent assay (ELISA) plate after culturing for another 24 h, and the concentration of arginase was assessed following the instructions of the manufacturer (FANKEWEI, China). The absorbance at 450 nm and the arginase amount that was produced by the quantified RAW 264.7 cells were recorded by the multimode plate reader (EnVision, PerkinElmer).

4.9. Enzyme-Linked Immunosorbent Assay of IL-10. The concentrations of IL-10 were determined using available ELISA kits. In DMEM containing 10% FBS, macrophages (3.5×10^4 cells/mL) were treated with NPs for 24 h. The preparation of the control experiment was also done without the addition of NPs or NP-coronas using the same conditions. Then, the culture medium (100 μL) was transferred to the ELISA plate, which was assessed following the instructions of the manufacturer (R&D Systems). Using a multimode plate reader (EnVision, PerkinElmer), the cytokine levels were analyzed via a standard calibration curve.

4.10. Statistical Analysis. All data were reported as mean ± sd; $n = 3$ for the experiments. p Values were calculated using one-way or two-way analysis of variance (ANOVA) with Tukey's multiple comparisons to test the statistical significance between different groups using SPSS version 22.0 (SPSS Inc., Chicago). Significantly different values are indicated according to the following criteria: NS, not significant; *, $p < 0.05$; **, $p < 0.01$; and ***, $p < 0.001$.

AUTHOR INFORMATION

Corresponding Authors

Ling Han − *NMPA Key Laboratory for Research and Evaluation of Innovative Drug, Henan Key Laboratory of Organic Functional Molecule and Drug Innovation, Collaborative Innovation Center of Henan Province for Green Manufacturing of Fine Chemicals, School of chemistry and chemical engineering, Henan Normal University, Xinxiang, Henan 453007, China; Shanghai Medicilon Inc., Shanghai 201200, China*; Email: lhan@medicilon.com.cn

Huayan Yang − *NMPA Key Laboratory for Research and Evaluation of Innovative Drug, Henan Key Laboratory of Organic Functional Molecule and Drug Innovation, Collaborative Innovation Center of Henan Province for Green Manufacturing of Fine Chemicals, School of chemistry and*

https://doi.org/10.1021/acsomega.3c08288
ACS Omega 2024, 9, 27898−27905

chemical engineering, Henan Normal University, Xinxiang, Henan 453007, China; Shanghai Applied Radiation Institute, Shanghai University, Shanghai 200444, China; orcid.org/0000-0002-5086-9332;
Email: yanghy_1983@163.com

Authors

Yijing Wang − *NMPA Key Laboratory for Research and Evaluation of Innovative Drug, Henan Key Laboratory of Organic Functional Molecule and Drug Innovation, Collaborative Innovation Center of Henan Province for Green Manufacturing of Fine Chemicals, School of chemistry and chemical engineering, Henan Normal University, Xinxiang, Henan 453007, China*

Hongyan Jia − *NMPA Key Laboratory for Research and Evaluation of Innovative Drug, Henan Key Laboratory of Organic Functional Molecule and Drug Innovation, Collaborative Innovation Center of Henan Province for Green Manufacturing of Fine Chemicals, School of chemistry and chemical engineering, Henan Normal University, Xinxiang, Henan 453007, China*

Zhiqin Zhang − *NMPA Key Laboratory for Research and Evaluation of Innovative Drug, Henan Key Laboratory of Organic Functional Molecule and Drug Innovation, Collaborative Innovation Center of Henan Province for Green Manufacturing of Fine Chemicals, School of chemistry and chemical engineering, Henan Normal University, Xinxiang, Henan 453007, China*

Shouning Yang − *NMPA Key Laboratory for Research and Evaluation of Innovative Drug, Henan Key Laboratory of Organic Functional Molecule and Drug Innovation, Collaborative Innovation Center of Henan Province for Green Manufacturing of Fine Chemicals, School of chemistry and chemical engineering, Henan Normal University, Xinxiang, Henan 453007, China;* orcid.org/0000-0003-2981-6727

Fangxiao Li − *NMPA Key Laboratory for Research and Evaluation of Innovative Drug, Henan Key Laboratory of Organic Functional Molecule and Drug Innovation, Collaborative Innovation Center of Henan Province for Green Manufacturing of Fine Chemicals, School of chemistry and chemical engineering, Henan Normal University, Xinxiang, Henan 453007, China*

Fengfeng Li − *NMPA Key Laboratory for Research and Evaluation of Innovative Drug, Henan Key Laboratory of Organic Functional Molecule and Drug Innovation, Collaborative Innovation Center of Henan Province for Green Manufacturing of Fine Chemicals, School of chemistry and chemical engineering, Henan Normal University, Xinxiang, Henan 453007, China*

Complete contact information is available at:
https://pubs.acs.org/10.1021/acsomega.3c08288

Notes

The authors declare no competing financial interest.

■ ACKNOWLEDGMENTS

This work was financially supported by the National Natural Science Foundation of China (82073699 and 82130103), the National Key Research and Development Program of China (2022YFF0707205), the Natural Science Foundation of Henan (222300420055), and the Central Plains Scholars and Scientists Studio Fund (2018002).

■ REFERENCES

(1) Salvati, A.; Pitek, A. S.; Monopoli, M. P.; et al. Transferrin-functionalized nanoparticles lose their targeting capabilities when a biomolecule corona adsorbs on the surface. *Nat. Nanotechnol.* **2013**, *8*, 137−143.
(2) Walkey, C. D.; Olsen, J. B.; Song, F.; et al. Protein Corona Fingerprinting Predicts the Cellular Interaction of Gold and Silver Nanoparticles. *ACS Nano* **2014**, *8*, 2439−2455.
(3) Lundqvist, M. Tracking protein corona over time. *Nat. Nanotechnol.* **2013**, *8*, 701−702.
(4) Monopoli, M. P.; Åberg, C.; Salvati, A.; Dawson, K. A. Biomolecular coronas provide the biological identity of nanosized materials. *Nat. Nanotechnol.* **2012**, *7*, 779−786.
(5) Yang, H.; Wang, M.; Zhang, Y.; et al. Detailed insight into the formation of protein corona: Conformational change, stability and aggregation. *Int. J. Biol. Macromol.* **2019**, *135*, 1114−1122.
(6) Blunk, T.; Hochstrasser, D. F.; Sanchez, J. C.; Müller, B. W.; Müller, R. H. Colloidal carriers for intravenous drug targeting: plasma protein adsorption patterns on surface-modified latex particles evaluated by two-dimensional polyacrylamide gel electrophoresis. *Electrophoresis* **1993**, *14*, 1382−1387.
(7) Lundqvist, M.; Stigler, J.; Elia, G.; et al. Nanoparticle size and surface properties determine the protein corona with possible implications for biological impacts. *Proc. Natl. Acad. Sci. U.S.A.* **2008**, *105*, 14265−14270.
(8) Cedervall, T.; Lynch, I.; Foy, M.; et al. Detailed Identification of Plasma Proteins Adsorbed on Copolymer Nanoparticles. *Angew. Chem., Int. Ed.* **2007**, *46*, 5754−5756.
(9) Cedervall, T.; Lynch, I.; Lindman, S.; et al. Understanding the nanoparticle−protein corona using methods to quantify exchange rates and affinities of proteins for nanoparticles. *Proc. Natl. Acad. Sci. U.S.A.* **2007**, *104*, 2050−2055.
(10) Lundqvist, M.; Stigler, J.; Cedervall, T.; et al. The Evolution of the Protein Corona around Nanoparticles: A Test Study. *ACS Nano* **2011**, *5*, 7503−7509.
(11) Tenzer, S.; Docter, D.; Kuharev, J.; et al. Rapid formation of plasma protein corona critically affects nanoparticle pathophysiology. *Nat. Nanotechnol.* **2013**, *8*, 772−781.
(12) Corbo, C.; Molinaro, R.; Taraballi, F.; et al. Unveiling the in Vivo Protein Corona of Circulating Leukocyte-like Carriers. *ACS Nano* **2017**, *11*, 3262−3273.
(13) Ritz, S.; Schöttler, S.; Kotman, N.; et al. Protein corona of nanoparticles: distinct proteins regulate the cellular uptake. *Biomacromolecules* **2015**, *16*, 1311−1321.
(14) Bisker, G.; Dong, J.; Park, H. D.; et al. Protein-targeted corona phase molecular recognition. *Nat. Commun.* **2016**, *7*, No. 10241.
(15) Lara, S.; Alnasser, F.; Polo, E.; et al. Identification of Receptor Binding to the Biomolecular Corona of Nanoparticles. *ACS Nano* **2017**, *11*, 1884−1893.
(16) Ke, P. C.; Lin, S.; Parak, W. J.; Davis, T. P.; Caruso, F. A Decade of the Protein Corona. *ACS Nano* **2017**, *11*, 11773−11776.
(17) Francia, V.; Yang, K.; Deville, S.; et al. Corona Composition Can Affect the Mechanisms Cells Use to Internalize Nanoparticles. *ACS Nano* **2019**, *13*, 11107−11121.
(18) Yang, H.; Lu, S.; Wang, S.; et al. Evolution of the protein corona affects macrophage polarization. *Int. J. Biol. Macromol.* **2021**, *191*, 192−200.
(19) Lunov, O.; Syrovets, T.; Loos, C.; et al. Differential uptake of functionalized polystyrene nanoparticles by human macrophages and a monocytic cell line. *ACS Nano* **2011**, *5*, 1657−1669.
(20) Fuchs, A. K.; Syrovets, T.; Haas, K. A.; et al. Carboxyl- and amino-functionalized polystyrene nanoparticles differentially affect the polarization profile of M1 and M2 macrophage subsets. *Biomaterials* **2016**, *85*, 78−87.
(21) Vu, V. P.; Gifford, G. B.; Chen, F.; et al. Immunoglobulin deposition on biomolecule corona determines complement opsonization efficiency of preclinical and clinical nanoparticles. *Nat. Nanotechnol.* **2019**, *14*, 260−268.

(22) Cai, R.; Ren, J.; Ji, Y.; et al. Corona of Thorns: The Surface Chemistry-Mediated Protein Corona Perturbs the Recognition and Immune Response of Macrophages. *ACS Appl. Mater. Interfaces* **2020**, *12*, 1997−2008.
(23) Duncan, B.; Kim, C.; Rotello, V. M. Gold nanoparticle platforms as drug and biomacromolecule delivery systems. *J. Controlled Release* **2010**, *148*, 122−127.
(24) Fratoddi, I. Hydrophobic and Hydrophilic Au and Ag Nanoparticles. Breakthroughs and Perspectives. *Nanomaterials* **2018**, *8*, 1−25.
(25) Tian, L.; Zhao, W.; Li, L.; et al. Multi-talented applications for cell imaging, tumor cells recognition, patterning, staining and temperature sensing by using egg white-encapsulated gold nanoclusters. *Sens. Actuators, B* **2017**, *240*, 114−124.
(26) Yang, H.; Wang, M.; Zhang, Y.; et al. Conformational-transited protein corona regulated cell-membrane penetration and induced cytotoxicity of ultrasmall Au nanoparticles. *RSC Adv.* **2019**, *9*, 4435−4444.
(27) Huang, X.; Jain, P. K.; El-Sayed, I. H.; El-Sayed, M. A. Plasmonic photothermal therapy (PPTT) using gold nanoparticles. *Lasers Med. Sci.* **2008**, *23*, 217−228.
(28) Huang, X.; El-Sayed, M. A. Gold nanoparticles: Optical properties and implementations in cancer diagnosis and photothermal therapy. *J. Adv. Res.* **2010**, *1*, 13−28.
(29) Mendes, R.; Pedrosa, P.; Lima, J. O. C.; Fernandes, A. R.; Baptista, P. V. Photothermal enhancement of chemotherapy in breast cancer by visible irradiation of Gold Nanoparticles. *Sci. Rep.* **2017**, *7*, No. 10872.
(30) Kim, H. S.; Lee, D. Y. J. Photothermal therapy with gold nanoparticles as an anticancer medication. *J. Pharm. Invest.* **2016**, *47*, 19−26.
(31) Wang, H.; Zheng, L.; Guo, R.; et al. Dendrimer-entrapped gold nanoparticles as potential CT contrast agents for blood pool imaging. *Nanoscale Res. Lett.* **2012**, *7*, No. 190.
(32) Rachela; Agrawal, A.; Kotov, N. A.; et al. Targeted Gold Nanoparticles Enable Molecular CT Imaging of Cancer. *Nano Lett.* **2008**, *8*, 4593−4596.
(33) Tan, J.; Cho, T. J.; Tsai, D. H.; et al. Surface Modification of Cisplatin-Complexed Gold Nanoparticles and Its Influence on Colloidal Stability, Drug Loading, and Drug Release. *Langmuir* **2018**, *34*, 154−163.
(34) Williams; Zee, J. *Preparation of Gold Nanoparticle-Cisplatin Conjugates and Investigation of their Toxicity in Zebrafish*, Senior Projects Spring 2014; Bard, 2014.
(35) Gordon, S.; Taylor, P. R. Monocyte and macrophage heterogeneity. *Nat. Rev. Immunol.* **2005**, *5*, 953−964.
(36) Rodell, C. B.; Arlauckas, S. P.; Cuccarese, M. F.; et al. TLR7/8-agonist-loaded nanoparticles promote the polarization of tumor-associated macrophages to enhance cancer immunotherapy. *Nat. Biomed. Eng.* **2018**, *2*, 578−588.
(37) Beatty, G. L.; Chiorean, E. G.; Fishman, M. P.; et al. CD40 Agonists Alter Tumor Stroma and Show Efficacy Against Pancreatic Carcinoma in Mice and Humans. *Science* **2011**, *331*, 1612−1616.
(38) Yang, H.; Yang, S.; Kong, J.; Dong, A.; Yu, S. Obtaining information about protein secondary structures in aqueous solution using Fourier transform IR spectroscopy. *Nat. Protoc.* **2015**, *10*, 382−396.
(39) Marklein, R. A.; Lam, J.; Guvendiren, M.; Sung, K. E.; Bauer, S. R. Functionally-Relevant Morphological Profiling: A Tool to Assess Cellular Heterogeneity. *Trends Biotechnol.* **2018**, *36*, 105−118.
(40) Rodell, C. B.; Arlauckas, S. P.; Cuccarese, M. F.; et al. TLR7/8-agonist-loaded nanoparticles promote the polarization of tumor-associated macrophages to enhance cancer immunotherapy. *Nat. Biomed. Eng.* **2018**, *2*, 578−588.
(41) McWhorter, F. Y.; Wang, T.; Nguyen, P.; Chung, T.; Liu, W. F. Modulation of macrophage phenotype by cell shape. *Proc. Natl. Acad. Sci. U.S.A.* **2013**, *110*, 17253−17258.
(42) Lawrence, T.; Natoli, G. Transcriptional regulation of macrophage polarization: enabling diversity with identity. *Nat. Rev. Immunol.* **2011**, *11*, 750−761.
(43) Jana, N. R.; Gearheart, L.; Murphy, C. J. Wet Chemical Synthesis of High Aspect Ratio Cylindrical Gold Nanorods. *J. Phys. Chem. B* **2001**, *105*, 4065−4067.
(44) Wang, C.; Chen, B.; He, M.; Hu, B. Composition of Intracellular Protein Corona around Nanoparticles during Internalization. *ACS Nano* **2021**, *15*, 3108−3122.
(45) Hou, D.; Zhang, L.; Deng, F.; et al. Comparative proteomics reveal fundamental structural and functional differences between the two progeny phenotypes of a baculovirus. *J. Virol.* **2013**, *87*, 829−839.
(46) Walkey, C. D.; Olsen, J. B.; Guo, H.; Emili, A.; Chan, W. C. W. Nanoparticle Size and Surface Chemistry Determine Serum Protein Adsorption and Macrophage Uptake. *J. Am. Chem. Soc.* **2012**, *134*, 2139−2147.
(47) Cho, E. C.; Xie, J.; Wurm, P. A.; Xia, Y. Understanding the Role of Surface Charges in Cellular Adsorption versus Internalization by Selectively Removing Gold Nanoparticles on the Cell Surface with a I-2/KI Etchant. *Nano Lett.* **2009**, *9*, 1080−1084.
(48) Granger, D. L.; Taintor, R. R.; Boockvar, K. S.; Hibbs, J. B., Jr. Measurement of nitrate and nitrite in biological samples using nitrate reductase and Griess reaction. *Methods Enzymol.* **1996**, *268*, 142−151.

https://doi.org/10.1021/acsomega.3c08288
ACS Omega 2024, 9, 27898−27905